Orientational order in random packings of ellipses

B. J. Buchalter and R. Mark Bradley
Department of Physics, Colorado State University, Fort Collins, Colorado 80523
(Received 4 May 1992)

By means of Monte Carlo simulations, we examine the behavior of random packings of hard ellipses formed by pouring into a two-dimensional container. The particles pack so that their semimajor axes are preferentially aligned with the horizontal, and their orientational alignment increases with increasing aspect ratio. This self-organizational effect is accompanied by a corresponding reduction in the translational order of the centers of masses of the particles. For sufficiently elongated particles no translational order is present: The packings are amorphous, but still exhibit long-range orientational order. We call this state a "nematic glass." We find that the orientational order also increases as the rate of deposition is reduced. The orientational order decreases if the packings are shaken. The behavior of the packings can be explained heuristically as being the result of competition between two local-potential-energy-minimization processes. The relevance of our results to materials science and petroleum engineering is discussed.

PACS number(s): 05.40.+j, 81.35.+k, 81.20.Ev

I. INTRODUCTION

There has recently been considerable interest in random packings of particles in two and three dimensions. Random packings of disks (in two dimensions) and spheres (in three dimensions) were at first constructed under the influence of a central potential to model liquid structure [1,2]. As work progressed, it was realized that these systems comprised a better model of amorphous materials than of liquids [3,4]. More recently, random packings constructed in the influence of a uniform gravitational field have become the object of scrutiny. These packings are used to model the macroscopic arrangement of granules in powders and porous materials, and can be employed to make predictions about the porosity, structure, and stability of granular media [5,6]. This area is multidisciplinary in nature, providing insight into problems in physics, sedimentology, petroleum engineering, materials science, and process engineering.

In all likelihood, a random, closely packed metastable state will result when a collection of identical particles is poured into a container, rather than the regular "crystalline" arrangement in which the lowest energy is achieved. Significant work has been done towards characterizing the structure of these random packings over the past two decades. Initial work was directed towards the definition and analysis of random monodisperse sphere and disk packings. Berryman has shown that there is a distinction to be made in three dimensions between loose and close random packings, but in two dimensions the distinction is not as clear [7]. There is also evidence that the random densely packed structure of disks in two dimensions may be unstable [7]. As a result, it may be that in two dimensions, by applying a suitable set of perturbations, a random dense packing can be reduced to a crystalline array. In contrast to the two-dimensional (2D) case, three-dimensional (3D) packings of spheres form stable dense random packings. The difference is that the 3D system exhibits frustration, while the 2D system does not. Simply stated, frustration is a result of competition between local and global minimization of potential energy [8].

An algorithm introduced by Visscher and Bosterli to construct packings of spherical particles in the influence of a uniform gravitational field has the benefit of being fast enough that large systems can be constructed [9]. In the Visscher-Bosterli model, spheres are dropped one at a time and fall straight down from random release points above the packing. Once a particle has reached the surface of the aggregate, it rolls without slipping along the surface until it reaches a point of mechanical stability. It then moves no further. The Visscher-Bosterli model is strictly valid only in the limit of zero deposition rate since there is no interaction between the particles during deposition. Moreover, because the particles are frozen in place once they have reached a stable resting place, the model does not allow for collective motion within the packing. Since the particles are dropped from random positions, the packings have a random character.

Real systems are composed of particles that are polydisperse [10]. Even if random deposition of monodisperse spheres (or disks) could form a crystalline packing, a polydisperse distribution of sizes will destroy that possibility [11]. Also, if the smallest particles are smaller than the pores in between the larger particles, the small particles will pack within the pores of the large particle packing, leading to a much larger overall packing fraction [12]. Most of the work that preceded that of Visscher and Bosterli dealt with monodisperse spheres (or disks). In order to examine the effect of polydispersity, Visscher and Bosterli also constructed a packing with a range of disk sizes.

Visscher and Bosterli attempted to simulate shaking by dropping an ensemble of particles at each step and choosing the particle that had the minimum potential energy. This accomplishes the goal of forcing the packing to form a more dense, lower total potential-energy packing, but

ignores the fact that shaking is a complex dynamic process and that particle interactions during relaxation are important. In particular, if one shakes a random packing composed of spheres of more than one size, size segregation takes place [13]. The Visccher-Bosterli model exhibits no such effect. In order to overcome these difficulties, Rosato *et al.* performed a Monte Carlo simulation of pouring and shaking that treats each macroscopic particle as an independent random walker in a gravitational field [14,15]. This model allows for particle interactions during relaxation, and can be used to examine the time evolution of the aggregate during shaking. Another example of the importance of particle interactions is found in the flow of elongated particles in a gravitational field. In a cellular automaton model of such a granular flow, the particles tend to flow with their long axes along the vertical [16].

We see that as work has progressed, refinements have been added to the original model of monosized spheres packed in a gravitational field. It was recognized that in real systems the particles are not all the same size and that this fact has a significant effect on the properties of the packings. Particle interactions also play an important role in determining the properties of the aggregates. However, most models with these improvements still use spheres or disks as the constituent particles.

It has long been known that for most granular media the particles are not identical spheres. For example, sandstones are formed from particles with a variety of shapes and sizes [10]. Since sandstones are important reservoirs for oil, water, and natural gas, the porosity of these packings is of great economic importance [17]. Empirical studies have shown that the porosity of a packing depends on both the shapes and sizes of the particles that compose the packing [18]. In ceramics processing and metallurgy, a wide range of materials are formed by sintering powders composed of polydisperse aspherical particles [19]. Finally, it has recently been shown that granular conducting polymers can be formed from aspherical dispersions [20–24]. In the case of polyaniline [23,24], the polymer microparticles are prolate ellipsoids. In short, there are a range of granular materials in which the granules are aspherical. Despite this fact, random packings of aspherical particles have received only limited theoretical attention [25,26].

In this paper we present the results of our Monte Carlo simulations of freely rotating aspherical particles poured under the influence of gravity. The simplest perturbation to a sphere is the elongation of a preferred axis, which naturally forms an ellipsoid. Since our studies have been confined to two dimensions, we have worked with ellipses. We expect that much of the behavior in packings of aspherical particles will be affected by particle interactions during the pouring process. Indeed, as we shall see, the properties of these packings are strongly affected by the deposition rate. This suggests that we base our simulation method on the work of Rosato *et al.* rather than that of Visscher and Bosterli.

Our simulations show that the properties of packings depend strongly on the shape of the constituent particles. We find that for packings of identical ellipses, the ellipses exhibit orientational order and that the degree of orientational order depends on the aspect ratio, as well as the deposition rate. The final porosity of the aggregate is also dependent on the aspect ratio. The amount of translational order present decreases with increasing elongation. For particles with sufficiently large aspect ratio, the packings are amorphous but still exhibit orientational order. Finally, we find that, as with the shaking of spherical particles, the properties of packings of ellipses change with shaking. For polydisperse spherical packings, the packing goes from a uniform spatial distribution of sizes within the packing to a size-segregated distribution as shaking progresses. For ellipses, the orientational order decreases with shaking.

The paper is organized as follows: In Sec. II we describe our pouring algorithm in detail and explain our methods of analysis. The results of our simulations are presented and discussed in Sec. III. In Sec. IV we give our conclusions and suggest directions for future work.

II. COMPUTATIONAL METHOD

In this paper we describe the results of our simulations of the concurrent deposition of a relatively large number of two-dimensional elliptical particles in a box. All of the particles are identical. The ellipses are taken to have semimajor axis with unit length, and aspect ratio α defined by

$$\alpha \equiv \frac{(\text{semimajor axis length})}{(\text{semiminor axis length})} .$$

Naturally, with this definition, α is always greater than or equal to 1. The simulation program keeps track of the center-of-mass location of each particle, and the angle θ that its semimajor axis makes with the x axis.

To simplify the simulations, we discretized the particle positions and orientations. The centers of mass are represented by points on a square lattice or grid. The lattice spacing is chosen to be small enough that the discretization does not significantly alter the properties of the final packings, but large enough that the simulations run in a reasonable amount of time. The orientations of the particles are chosen to be integral multiples of $2\pi/N_\theta$. Here, N_θ is the number of orientations the particles can assume. Again, N_θ is chosen so that the properties of the packings do not change significantly as we increase N_θ. For all of the results presented here, the semimajor axis is 32 grid units long, and $N_\theta=60$. As a check, we examined packings with semimajor-axis length 64 and $N_\theta=120$. The results are essentially the same as obtained using our usual discretization. To show that our results on orientational order are not due to the fact that $\theta=0$ is one of the allowed angles in the discretization, we also examined packings with angular discretizations of the form $\theta=(2\pi/N_\theta)n_\theta+(\pi/N_\theta)$, where $n_\theta=0,1,\ldots,N_\theta-1$. We find that the properties of the final packing are not significantly altered.

Our simulation method is based on the technique introduced by Rosato *et al.* [14,15] in their simulation of the pouring and shaking of disks. We begin by randomly placing N particles in a box. The size of the box is chosen

so that the final packing will be roughly square, and so that the average density of the initial distribution of particles is γ. Since the particles are placed randomly and uniformly, γ is simply the fraction of the total box area covered by the particles. In a real experiment it would be difficult to arrange the particles randomly in a vertical box and then allow them to fall. A more likely scenario would be to pour particles into the top of a box at a given rate. The parameter γ can be thought of as being analogous to the rate of pouring. The walls of the box are taken to limit the motion of the centers of mass of the particles but not their orientation. These boundary conditions are discussed in detail below. The particles are randomly distributed within the volume of the box with the constraint that the great circles of the particles may not overlap, i.e., the centers of mass of each pair of particles must be separated by a distance of at least 1. Therefore, there are absolutely no orientational correlations at time $t=0$.

After all of the particles have been placed within the simulation volume, the pouring procedure begins. The pouring is simulated using a variant of the Monte Carlo method [27]. In the standard Monte Carlo algorithm we would start by randomly choosing a particle, and then randomly choosing a translation vector and an angle to rotate the particle through. Next, we would compute the change in energy and hence the probability of accepting the trial move. Since the particles are macroscopic and the temperature is taken to be comparable to room temperature, we exclude all upward movements of the particle, and accept all downward movements with equal probability [15]. As a result, we may simply choose our translation vector so that the z coordinate of the particle will decrease or stay the same. In the standard algorithm, if the new position and orientation do not cause an overlap, we move the particle into the new configuration. However, if we simply move the particle to its new position and orientation, we introduce the possibility of "jumping" over a forbidden configuration and arriving at a configuration that is allowed, but unreachable. The probability of generating a forbidden "jump" increases rapidly with increasing aspect ratio. To avoid this possibility, we instead "propagate" the particle through the system.

To propagate the particle, we compute the angular velocity needed to place the particle in the correct final orientation when its center of mass reaches its final position [28]. The sense of the rotation is randomly chosen. We take advantage of the fact that the positions and the orientations of the particles are discretized by requiring that the particle does not change either its angle or its center-of-mass position by more than one discretization step at a time.

We continue stepping the particle along the trajectory, one grid point at a time, until the particle collides with another object, collides with one of the walls, or reaches the maximum translation distance. If a collision occurs, the particle is restored to the position it had just before the collision and the propagation is ended.

The walls in our simulations are defined in order to reduce the finite-size effects on the orientational order.

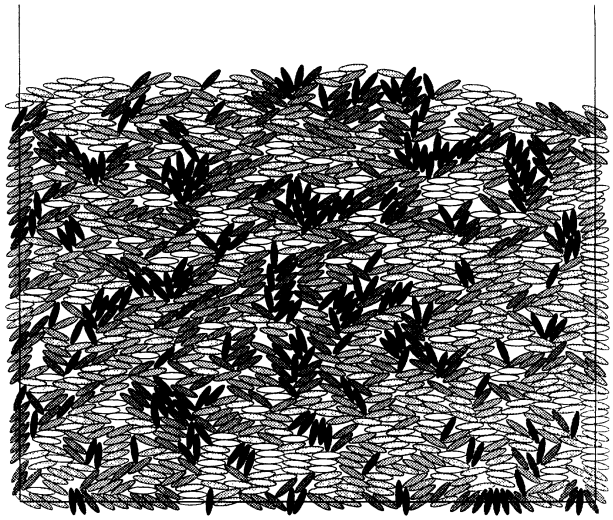

FIG. 1. A packing of 1200 ellipses with $\alpha=4$. The shading of each particle is proportional to $|\theta-\pi/2|$, where $\theta=\pi/2$ is represented by black and $\theta=0$ is represented by white. This shading makes it easier to see oriented domains. The initial density in this simulation was $\gamma=0.25$.

We require the centers of mass to remain within the box, but permit the orientation of a particle in contact with a wall to be arbitrary. This means that there is no forced alignment between the walls of the box and the long axis of the particles. Figure 1 is a representative packing for $\alpha=4$ particles with these boundary conditions. Collisions with other particles are detected by means of an overlap criterion. We employ the Vieillard-Baron criterion [29], which is an analytic test that reveals whether two ellipses intersect. In all of our simulations the maximum translation distance was taken to be three times the semimajor axis length. We choose this length to limit a single particle to motion within its local environment before being rerandomized, and yet still allow a reasonable rate of propagation. Increasing the maximum translation distance is similar in effect to increasing the pouring rate, and the role of the pouring rate is discussed in detail below.

We continue to move the particles using the algorithm just described until the system is close to a metastable state. Figure 2 shows the total potential energy as a function of the number of attempted moves for a test run of 3×10^6 attempted moves. The total potential energy of the system is within 0.7% of its asymptotic value by the 1×10^6 attempted move. In all the simulations that follow, we simply end the simulation after the 1×10^6 attempted move.

When we began this study, we determined overlaps by a bitmap criterion which turned out to be unreliable. This method explicitly uses the fact that space and angles are discretized. We computed a set of bitmaps to represent the ellipses at each of the discretized angles. The bitmap is simply an object that contains a binary "true" for each element of the grid that is within the interior of the ellipse. By using fast logical operations, we

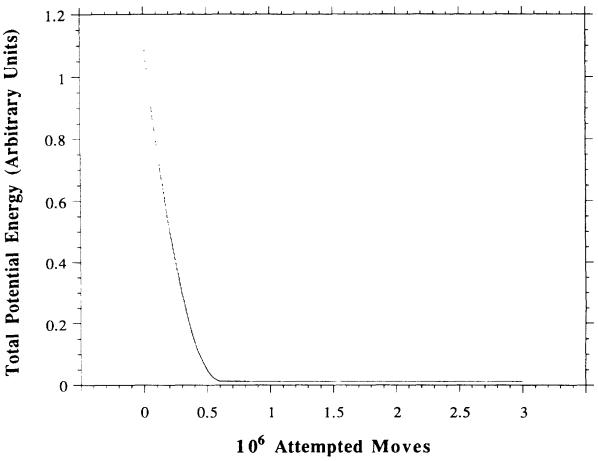

FIG. 2. The total potential energy as a function of the number of attempted moves for the simulation that yielded the packing shown in Fig. 1. The total potential energy has come close to its asymptotic value by the 1×10^6 attempted move.

could determine whether two ellipses overlap.

One attractive aspect of the bitmap method is that it allows us to construct packings of particles with arbitrary shapes. However, it turns out that the discretized-overlap criterion has an inherent difficulty. When a curved object is discretized onto a square lattice the object will still be, to a good approximation, curved. However, the discretization introduces flat edges near the points along the curve where the curve is tangential to a lattice direction. This phenomenon has the effect of converting the curved object into an approximately curved object with a number of flat edges. Although this approximate object behaves similarly to the original object for the most part, there are some significant differences. In particular, a discretized ellipse may stand on end. We must consider the bitmaps to be an unreliable representation of a real, continuously curved object. As a result, we have used the Vieillard-Baron criterion to generate all of the results presented here.

In order to simulate pouring and shaking, we begin by creating a packing by pouring the particles into a box using the above procedure. After the pouring process has been completed, we simulate a vertical shake by rigidly translating the entire packing upwards by a specified amplitude and then quickly lowering the entire box back to its original position. Finally, we perform a Monte Carlo simulation of the particles' fall to the base of the container using the same rules that we use to pour the particles into the box. The only difference between a pouring simulation and the pouring phase of a shaking simulation is the initial state of the packing.

In analyzing the orientational order in our packings, we have found two techniques to be of particular utility. First, we define the orientational order parameter. This allows us to assign a single number to a given packing that indicates how much orientational order is present. The order parameter that we have defined is

$$\mathcal{Q}\equiv\frac{1}{N}\sum_{i=1}^{N}\cos(2\theta_i)\ . \tag{1}$$

Here, N is the number of particles in the packing and θ_i is the angle of the ith particle. Because $\cos(2\theta)$ is symmetric about $\theta=\pi/2$, each particle contributes to $\mathcal{Q}$ according to its absolute angular displacement from the vertical without regard to the sense of the displacement. This means that a particle that is leaning an angle ϕ to the right of vertical contributes the same as a particle that is leaning ϕ to the left of vertical. Note that a uniform distribution of angles will result in $\mathcal{Q}=0$, while, if all particles lie flat, $\mathcal{Q}=1$.

We will also make histograms of the particle population versus the folded angle. The folded angle is given by

$$\theta^f\equiv\begin{cases}\theta & \text{for } 0\le\theta<\pi/2\\ \theta-\pi & \text{for } \pi/2\le\theta<3\pi/2\\ \theta-2\pi & \text{for } 3\pi/2\le\theta<2\pi\ .\end{cases}$$

Rotating an ellipse by π radians about its center of mass gives us the same ellipse, and we use the folded angle to correctly account for this fact. Using the folded angle has the effect of folding the angles into the range $[-\pi/2,\pi/2)$. To form the histogram, we count the number of particles whose angles fall between the top and the bottom of a given bin. Finally, we plot this distribution. This allows us to visually inspect the angular distribution of particles for peaks. The presence of a peak indicates that there is a preferred orientation.

In order to characterize the degree of translational order in the packings, we compute the structure factor of the centers of the particles. The structure factor is defined as

$$S(\mathbf{k})\equiv\frac{1}{2\pi}\left|\int d^2x\,\rho(\mathbf{x})e^{i\mathbf{k}\cdot\mathbf{x}}\right|^2, \tag{2}$$

where

$$\rho(\mathbf{x})\equiv\sum_{i=1}^{N}\delta(\mathbf{x}-\mathbf{x}_i)\ ,$$

and $\mathbf{x}_i$ is the center-of-mass position of the ith particle in the packing for $i\in\{1,\ldots,N\}$. $S(\mathbf{k})$ is proportional to the intensity pattern that one would obtain if one performed a scattering experiment on the centers of mass of the particles. Several types of scattering patterns can result from this calculation. A pattern with well-defined spots arranged in a lattice corresponds to a crystal with long-range-order. Rings can also occur, in which case the packing is polycrystalline (Fig. 3). Finally, the intensity pattern can exhibit no structure whatsoever, and this corresponds to an amorphous packing (Fig. 4).

As we will see, our packings have scattering intensities that can be classified as either polycrystalline or amorphous. The scattering pattern depends on the aspect ratio of the ellipses α and their initial density γ. To determine the crystallite size within the polycrystalline packings, we take the scattering intensity averaged over all angles,

$$I(k)\equiv\frac{1}{2\pi}\int_0^{2\pi}d\theta_k S(k,\theta_k)\ ,$$

and plot it as a function of the magnitude of the wave

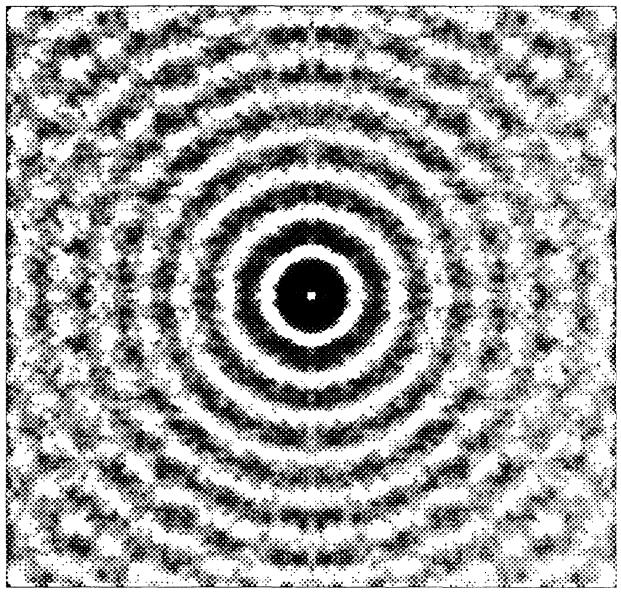

FIG. 3. The scattering pattern for a typical packing of 600 disks. The rings indicate that the packing is polycrystalline. The initial density in this simulation was $\gamma=0.25$.

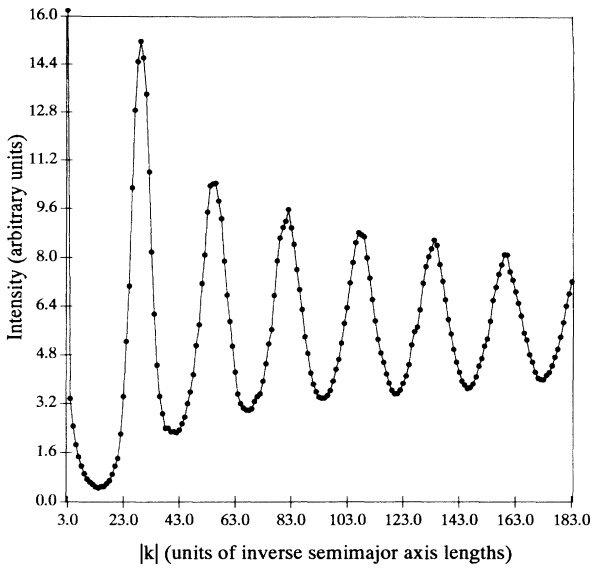

FIG. 5. The scattering intensity $I(k)$ (arbitrary units) plotted vs k. This is the intensity from the scattering pattern shown in Fig. 3. The crystallite size of the packing is proportional to the inverse of the width of the first peak.

vector $k\equiv|\mathbf{k}|$. This always leads to a radial scattering pattern with a peak at small values of k (Fig. 5). In order to compute a crude estimate of the full width at half maximum of this peak, we fit the top of the peak to a quadratic. We fit the quadratic to the points in the peak that have an intensity that is greater than the average of the maximum intensity of the peak and the next minimum.

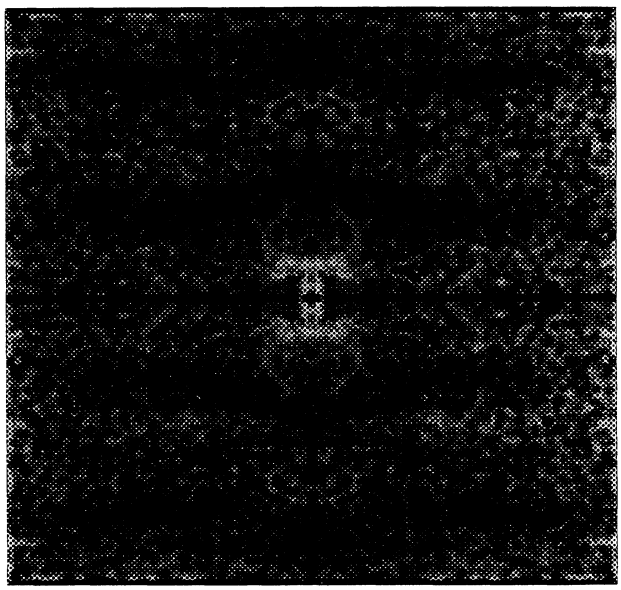

FIG. 4. The scattering pattern for a typical packing of 600 ellipses with aspect ratio $\alpha=8$. This scattering pattern has no structure, indicating that the packing is amorphous. The initial density in this simulation was $\gamma=0.25$.

Δk is the full width of the quadratic at half of the maximum intensity. Then,

$$\Delta x=2\pi/\Delta k \tag{3}$$

is a reasonable estimate of the average diameter of a crystallite in the packing.

Also of interest is the packing fraction η. The packing fraction is simply the area of the particles in the packing divided by the total area under the surface of the packing. Explicitly, η is defined by

$$\eta\equiv\frac{N\pi\alpha^{-1}}{W\sum_{n=0}h_n}\ . \tag{4}$$

Here, h_n is the highest point in the packing at the nth grid point along the x axis, and W is the width of the box in units of the grid lattice spacing.

III. RESULTS OF THE SIMULATIONS

We used the total potential energy to indicate when the packing has reached a metastable state. Although the total potential energy is the most obvious characteristic of the packing to monitor as a function of time, it is also rather uninteresting as a final result. Figure 6 shows $\mathcal{Q}$ for the test run as a function of the number of attempted moves. The orientational order parameter is the parameter of greatest interest and is close to its asymptotic value when we halt the simulation. In fact, $\mathcal{Q}$ is within 1% of its asymptotic value at the 1×10^6 attempted move.

The orientational order parameter has attained a stable, nonzero value at the termination of the simulation. This indicates that the packing has a nonuniform distribution angle. In order to establish that long-range

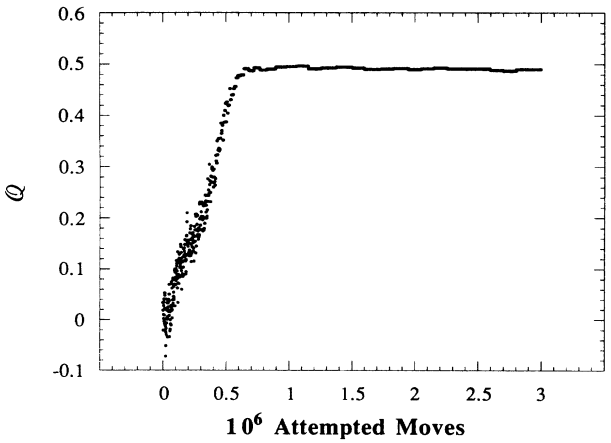

FIG. 6. The orientational order parameter $\mathcal{Q}$ as a function of the number of attempted moves for the packing shown in Fig. 1. As for the total potential energy (Fig. 2), $\mathcal{Q}$ has settled down to its asymptotic value by the 1×10^6 attempted move. Note that the initial state has $\mathcal{Q}$ close to zero since the particles' angles are initially randomly and uniformly distributed.

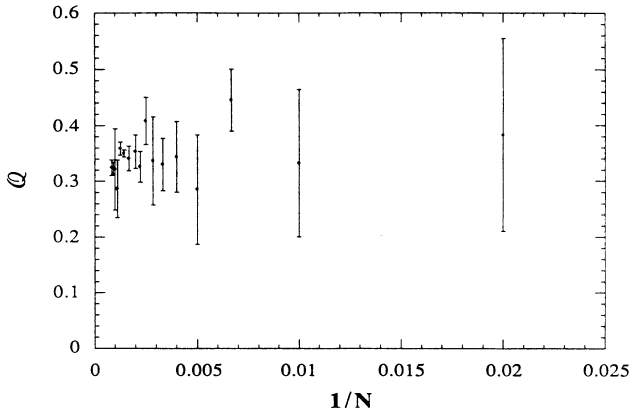

FIG. 8. The orientational order parameter $\mathcal{Q}$ as a function of $1/N$ for $\alpha=4$ and $\gamma=0.25$. The points are averaged over six simulations for $N<800$. For $N>800$ the points are averaged over four simulations.

orientational order is present, we also need to show that this distribution is peaked and that the effect does not go away as we increase the system size. Figure 7 shows a typical angular distribution of particles for a large packing of $\alpha=4$ particles. The distribution is strongly peaked about $\theta=0$, which indicates that the packing contains a significant number of particles aligned or nearly aligned with the horizontal. Figure 7 also shows that there are no other preferred orientations.

Figure 8 shows the orientational order parameter $\mathcal{Q}$ as a function of $1/N$ for $\alpha=4$ and $\gamma=0.25$. We note that although the results are somewhat noisy, there does not seem to be a significant trend. $\mathcal{Q}$ almost certainly does not tend to zero as $N\rightarrow\infty$. It appears that the finite orientational order parameter we observe is not merely a finite-size effect, and we can be confident that the orientational order persists in the limit $N\rightarrow\infty$.

Figure 9 shows a packing formed in a box with a random, jagged bottom. Although $\mathcal{Q}$ is different for this packing than for a similar packing in a box with a flat bottom, it is still nonzero. We also observe that the num-

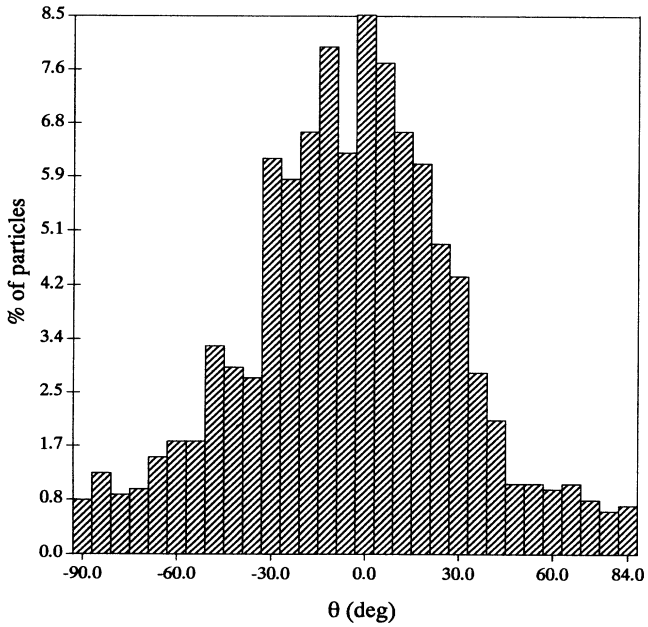

FIG. 7. Histogram of the particle population for each discretized angle θ. This histogram is for the packing illustrated in Fig. 1. The angle $\theta=0$ corresponds to particles aligned with the horizontal. The peak about zero indicates that the particles' semimajor axes are preferentially aligned with the horizontal.

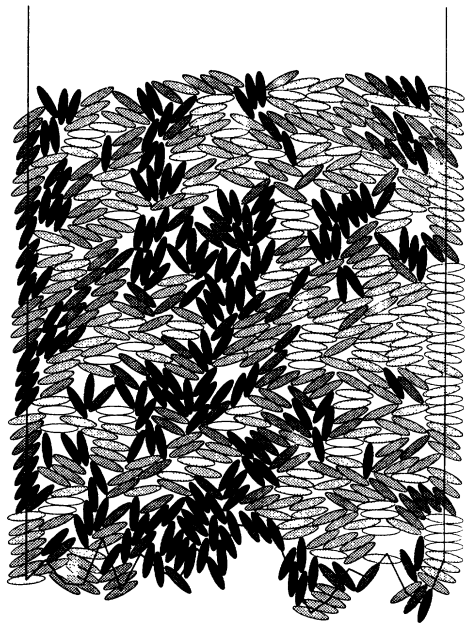

FIG. 9. A packing of 600 particles with $\alpha=4$ in a box with a piecewise linear random bottom. $\mathcal{Q}$ in 0.254 for this packing. The initial density in this simulation was $\gamma=0.1726$.

ber of particles that lay flat increases as we move up in the packing. This indicates that the dependence on the shape of the bottom is merely a finite-size effect. In particular, the orientational order we observe in packings constructed in rectangular boxes is not merely a result of the fact that the bottom of the box is horizontal.

As the system increases in size, the large-scale fluctuations in the surface height will increase in magnitude, and we might expect the orientational order to be disrupted. However, in the limit that the system becomes large and $\gamma \to 0$, the system has perfect orientational order, even though the surface exhibits large-scale fluctuations. This indicates that large-scale surface fluctuations have little effect on the orientational order. In fact, it is the small-scale fluctuations (the fluctuations on the order of the size of a particle) that most strongly effect the orientational order in the system.

We have demonstrated that $\mathcal{Q}$ is a good measure of the amount of orientational order present in these packings. From this point on we will use $\mathcal{Q}$ as our primary characterization of the final state of the packings.

We have attempted to determine the dependence of the orientational order on the aspect ratio α. As we will see, α is not the only parameter in the model that affects the orientational order of the final packing. The initial density γ is also important.

As a result of computer-time constraints, it was not feasible to map out the entire (α,γ) space. Instead, we decided to pick a particular value of γ and vary α. Similarly, we chose a particular value of α and varied γ.

Figure 10 illustrates the growth of the orientational order parameter $\mathcal{Q}$ with increasing aspect ratio α. Each point in the sequence shown in Fig. 10 corresponds to the average over five simulations with 600 particles each. The simulations were run with initial density $\gamma = 0.25 \pm 0.000\,05$ [30]. The sequence is for $\alpha = 32/n$, where n is an integer in the range $4, \ldots, 32$. It is clear from this figure that orientational order is augmented by increasing the aspect ratio of the particles involved in the pouring sequence, albeit only up to moderate aspect ratios, and then the increase in $\mathcal{Q}$ begins to saturate. We note that $\mathcal{Q} = 0$ for $\alpha = 1$, as expected.

It is easy to understand why $\mathcal{Q}$ is nonzero for $\alpha > 1$ and why it increases with increasing aspect ratio. Each particle "wants" to minimize its gravitational potential energy. This means that each particle would "like" to position its center of mass as low in the box as possible. As a first approximation, assume the particles fall one at a time onto a well-defined surface. Particle orientations other than horizontal incur a potential-energy "penalty." As we increase the aspect ratio, we increase this energy "penalty," and as a result, the particles are more likely to lay flat.

We can also understand why $\mathcal{Q}$ saturates at larger values of α. First, we must realize that pouring is a nonequilibrium, dynamic process. Our model does not allow for collective motion in the sense that one particle cannot cause another particle to move, and so each particle "tries" to minimize its own potential energy without regard to whether or not the global minimum will be reached. If the packing is in an intermediate state of the pouring process (a "partial packing"), and the partial packing is fairly dense and still settling, it is clearly in any given particle's "best interest" to have its semimajor axis parallel to gravity. This allows the particle to present the smallest cross-sectional area to the rest of the packing, so that it will be able to wiggle through small holes and better minimize its potential energy [31]. However, since the packing is fairly dense, the particles are not always free to realign their long axes parallel to **g**. As the packing finishes settling, the orientational disorder is partially frozen in. A larger aspect ratio will make turning parallel to gravity more favorable in a dense partial packing, because the change in cross-sectional area increases with increasing α. As α becomes large, the tendency of the particles to turn parallel to **g** prevents any further increase in $\mathcal{Q}$, and $\mathcal{Q}$ reaches a plateau.

As we see from Fig. 11, the orientational order parameter $\mathcal{Q}$ increases with decreasing γ. In particular, $\mathcal{Q}$ begins to grow at a value of γ that corresponds to a low enough initial density that the particles have very little

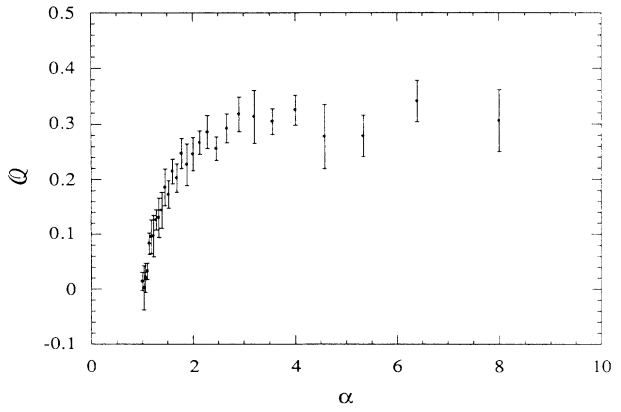

FIG. 10. A plot of the orientational order parameter $\mathcal{Q}$ as a function of the aspect ratio α. Each point is the average of five simulations of 600 particles. These simulations were run at constant initial density, $\gamma = 0.25 \pm 0.000\,05$.

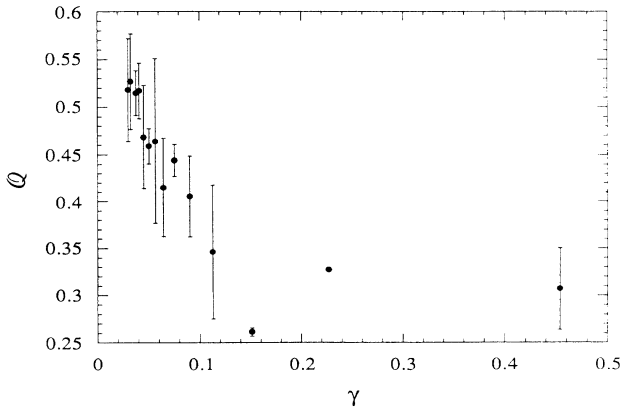

FIG. 11. The orientational order parameter $\mathcal{Q}$ as a function of initial density γ for aspect ratio $\alpha = 4$. Each point is an average over four simulations of 600 particles each.

interaction with each other as they fall. This means that on average, the particles hit the bottom of the box a few at a time. As γ decreases, the pouring becomes more and more like sequential deposition. In contrast to the dense partial packing described above, for small γ the particles are settled onto a well-defined surface. We see that for $\gamma \to 0$ our "first approximation" described above is realized. In this case, the goal of minimizing the single-particle potential energy is the same as minimizing the global potential energy. Each particle will align with the surface in order to minimize its own potential energy. The surface is relatively flat, and so each new particle added to the surface will tend to lay flat. Thus, as we decrease the initial density, we remove the competition described above and $\mathcal{Q}$ will tend to 1. We also expect that for smaller values of γ the plateau in the $\mathcal{Q}$-versus-α curve will be found at higher α.

Figure 12 shows the crystallite size Δx as a function of α. The crystallite size decreases rapidly with increasing aspect ratio, and so the packings composed of higher-aspect-ratio particles have less translational order. For $\alpha \lesssim 2$, the packings are polycrystalline. When $\alpha \gtrsim 2$, the crystallite size is less than the semimajor-axis length, and so the packings are "amorphous." To be precise, for $\alpha \gtrsim 2$ the centers of the particles have no translational order. In spite of this, there is long-range orientational order in the packings. We note that the crossover value $\alpha \approx 2$ is approximate, and should not be taken as exact.

In contrast to 3D sphere packings, the lack of translational order in 2D packings of ellipses cannot be attributed to frustration. This can be seen by taking a regular close packing of disks and stretching it along one of the lattice directions. By doing this we form a packing of ellipses for which the potential energy is a global minimum. The microparticles are arranged in a triangular lattice. The unit cell for the triangular lattice is the configuration for which the particles take up the least volume, and so this is the local-potential-energy minimum as well. Since the minimization of the local potential energy and the minimization of the global potential energy is compatible, there is no frustration. However, the reduction in the translational order with increasing aspect ratio can be readily understood. First of all, when we increase α, we decrease the energy penalty for stacking in a square lattice as compared to stacking in a close-packed triangular lattice. This means that the particles are more likely to form packings that are mixtures of the two different lattices. Secondly, for $\alpha > 1$, there is always some orientational disorder. For large α, small perturbations in the orientational order lead to large perturbations in translational order. The combination of these two effects quickly destroy the translational order as we increase α.

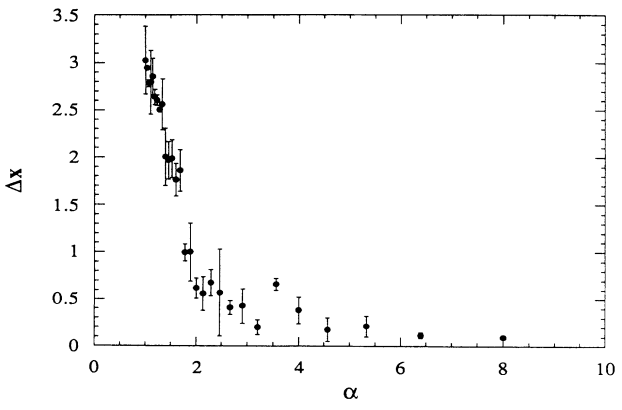

FIG. 12. The characteristic crystallite size Δx as a function of α. These data were obtained from the same set of simulations used to construct Fig. 10.

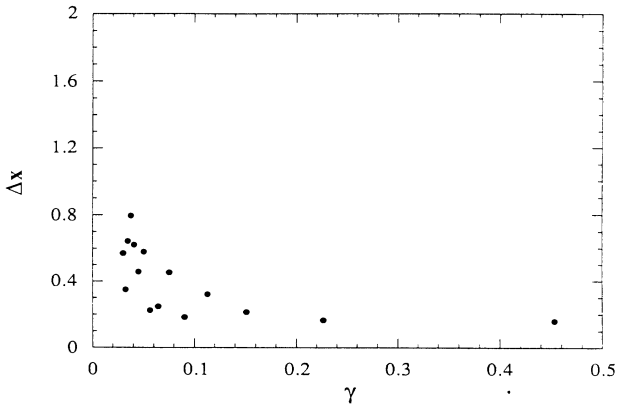

FIG. 13. The characteristic crystallite size Δx of the packings as a function of γ. These data were obtained from the same set of simulations used to construct Fig. 11.

When we examined the orientational order for packings with $\alpha = 4$ as a function of γ, we saw that the order increased with decreasing γ. Will we see a corresponding increase in the translational order if γ is decreased? The answer appears to be yes, as can be seen in Fig. 13. This indicates that random packings composed of high-aspect-ratio particles may form translationally ordered packings if deposited sufficiently slowly. However, in the regime that we studied, the crystallite size is still smaller than a single-particle semimajor-axis length.

A nematic liquid crystal is a system of rod-shaped molecules in which the centers of mass are randomly distributed (as in an ordinary liquid), but the long axes of the molecules are preferentially aligned along a certain direction [32]. Our packings are "glassy" for $\alpha \gtrsim 2$, and yet still exhibit long-range orientational order. In analogy to nematic liquid crystals, we propose calling an amorphous packing with orientational order a "nematic glass."

Figure 14 shows that the covering fraction η initially increases as a function of α, and then decreases sharply. There is much confusion in the literature as to how the porosity of a random packing depends on the shape of the constituent particles. It may be that this confusion is a direct result of the fact that the porosity is not a simple monotone function of α, and that different studies have examined different regimes [10,33,34].

The value $\eta = 0.76 \pm 0.02$ that we obtain for $\alpha = 1$ does not fall within the range of $0.82 \leq \eta \leq 0.84$ quoted by Berryman for random packings of disks. Moreover, Rosato

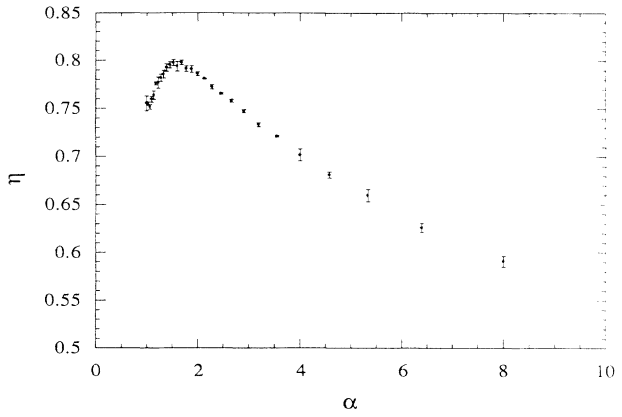

FIG. 14. The covering fraction η as a function of α. These data were obtained from the same set of simulations used to construct Fig. 10.

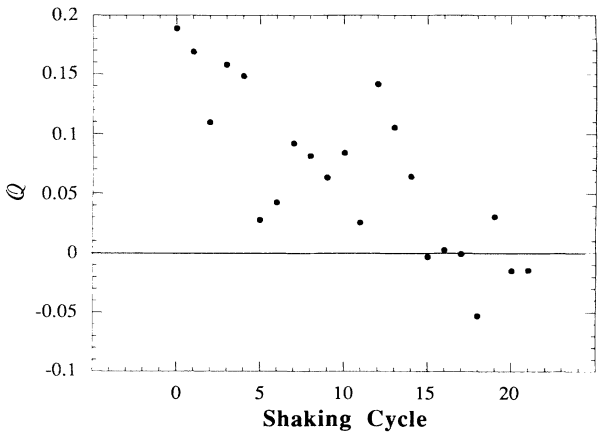

FIG. 16. $\mathcal{Q}$ for an aggregate of $\alpha=4$ particles as a function of shaking cycle for shaking amplitude $A=2$ semimajor-axis length. For this simulation, $\gamma=0.14$ and $N=400$.

et al. [14,15] obtained $\eta=0.81$ for their random disk packings. However, we know that the final properties of the packings are strongly dependent on the simulation dynamics, and so there is no inconsistency. In particular, since the spatial coordinates and angles are discretized and the particles do not "jump" in our simulations, our dynamics are not exactly the same as those used by Rosato *et al.* The discreteness of space has the effect of lowering the final packing fraction because the particles cannot necessarily get as close to each other as in a simulation in continuous space. By not allowing the particles to "jump," we further decrease the final packing fraction because we do not fill voids that a particle could "jump" into, but cannot propagate into.

Figure 15 shows the covering fraction η as a function of γ for $\alpha=4$. As we can see from this figure, the final covering fraction is not very sensitive to either the initial density γ or the exact final configuration of the packing, in direct contrast to $\mathcal{Q}$, which is sensitive to both. This lack of sensitivity is expected, because there are obviously an enormous number of configurations that have nearly the same potential energy.

Our preliminary results for the shaking of random packings of ellipses indicate that shaking of the aggregate reduces the orientational order present. Figure 16 shows $\mathcal{Q}$ for an aggregate of $\alpha=4$ particles as a function of shaking cycle for shaking amplitude $A=2$ semimajor-axis length, while Fig. 17 is for shaking amplitude $A=1$ semimajor-axis length. A larger shaking amplitude causes the orientational order to diminish more quickly. This is not surprising, because a larger shaking amplitude allows more movement, so that the packing can change its configuration faster. The reason for decreasing order in the aggregate is easily understood in terms of the competition between the particles' tendency to stand up on end and the tendency to lie flat. The tendency for a particle to stand up on end is strong in the dense partial packing formed during the shaking process. As a result, the system loses orientational order, and the more the system can change between each shaking cycle, the faster the system will lose orientational order.

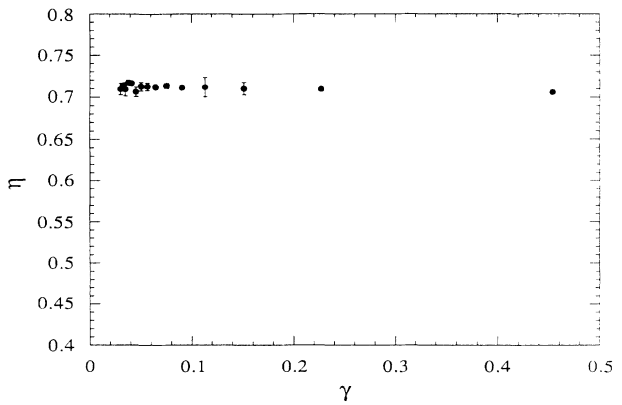

FIG. 15. The packing fraction η as a function of γ. These data were obtained from the same set of simulations used to construct Fig. 11.

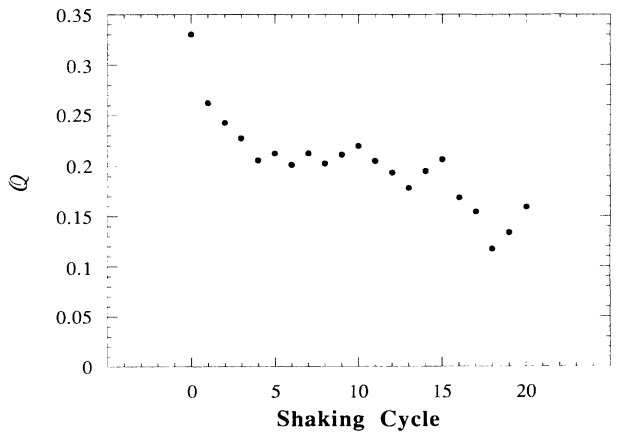

FIG. 17. $\mathcal{Q}$ for an aggregate of $\alpha=4$ particles as a function of shaking cycle for shaking amplitude $A=1$ semimajor-axis length. For this simulation, $\gamma=0.25$ and $N=600$.

IV. CONCLUSIONS

We have seen that pouring ellipses in a gravitational field forms a packing with a degree of orientational order. This order is self-imposed in that we did not individually manipulate the microparticles to form the aggregate. The degree of ordering grows with both increasing aspect ratio and decreasing initial density (or, more physically, decreasing pouring rate). Both of these effects can be understood in terms of local minimization of potential energy. The initial density controls how much interaction there is between particles as they settle. In the low-density, low-interaction limit the particles tend to align their long axes perpendicular to gravity as they fall to the surface of the aggregate. When the initial density is high, some particles will turn parallel to gravity in order to minimize the cross-sectional area presented to the rest of the particles. These two tendencies compete with each other as the initial density is increased. Decreasing the initial density removes the competition and increases the orientational order present in the packing.

We have also shown that the packings are polycrystalline in the $\alpha \rightarrow 1$ limit, and that the mean crystallite size swiftly decreases with increasing α. Since the aggregates are amorphous for $\alpha \gtrsim 2$, but nonetheless exhibit orientational order, we have dubbed these packings "nematic glasses."

Finally, our preliminary results indicate that shaking these aggregates tends to reduce the orientational order. Thus we can make a simple prescription for a materials scientist wishing to pack elongated objects in a way that will ensure the highest degree of orientational order: Deposit the objects as slowly as possible, and then disturb them as little as possible before you fix them in place.

There are a number of granular media composed of aspherical particles in which orientational order would be a desirable attribute. For example, recall that in the case of granular polyaniline the microparticles are prolate ellipsoids [23,24]. The polymer chains are believed to be aligned with the long axes of the polymer granules. As a result, these microparticles have large (approaching metallic) conductivities along their long axes, and are poor conductors along their short axes. If the long axes of microparticles could be aligned, the bulk material would have very high conductivity and would become an attractive candidate for a number of applications.

We close by discussing directions for future work. Two extensions to this work which would be quite interesting are 3D systems and more complicated particle shapes. We expect that particles with higher symmetry (e.g., polyhedra or rounded polyhedra) will, in general, exhibit more peaks in their angular distributions. In particular, one expects that packings of particles that have flat faces will exhibit peaks in the angular distributions corresponding to orientations in which a face is parallel to the horizontal. The strength of each peak will probably be related to the area of the corresponding face. We have done preliminary work with "spherocylinders" in two dimensions and find that the peaks are indeed localized about the orientations in which the flat edges are parallel to the horizontal. We also find that the peaks are narrower and stronger than the associated peak in the distribution for ellipses. Detailed results of this work are planned for a future paper.

We are currently extending our work to packings of aspherical particles in three dimensions. Even with simple objects like ellipsoids of revolution, the additional degree of freedom introduces a number of complications. We expect different types of ordering for prolate and oblate ellipsoids. For prolate ellipsoids, the long axis of the ellipsoid will tend to align with the horizontal, but its projection onto the x-y plane will be uniformly distributed. For oblate ellipsoids, the short axes should be preferentially aligned with $\mathbf{g}$. We plan to publish the results of a simulation of pouring ellipsoids in three dimensions in the future.

Clearly, more work needs to be done to understand the effect of shaking on packings of ellipses. We have presented preliminary results that suggest that, for packings of monodisperse ellipses, shaking decreases orientational order. We expect that size segregation will take place in packings of polydisperse ellipses, but the segregation velocities and low-shaking-amplitude behavior may be different than in packings of circles.

ACKNOWLEDGMENTS

We would like to thank J. Ariyasu, B. Berche, J.-M. Debierre, R. E. Eykholt, F. L. Galeener, C. S. Galovich, H. D. Hochheimer, L. Schwartz, P. N. Strenski, W. M. Visscher, and K. Wu for helpful discussions. This work was supported by U.S. National Science Foundation Grant No. DMR-9100257 and grants from Colorado State University and the Polymeric Materials Laboratory of the Colorado Advanced Materials Institute.

[1] J. l. Finney, Proc. R. Soc. London, Ser. A **319**, 479 (1970).
[2] G. D. Scott and D. M. Kilgour, J. Phys. D **2**, 863 (1969).
[3] C. H. Bennett, J. Appl. Phys. **43**, 2727 (1972).
[4] D. Turnbull and M. H. Cohen, Nature (London) **203**, 964 (1964).
[5] M. Shahinpoor, Powder Technol. **25**, 163 (1980).
[6] A. Mehta and S. F. Edwards, Physica A **157**, 1091 (1989).
[7] J. G. Berryman, Phys. Rev. A **27**, 1053 (1983).
[8] D. R. Nelson, Phys. Rev. B **28**, 5515 (1983).
[9] W. M. Visscher and M. Bosterli, Nature (London) **239**, 504 (1972).
[10] R. C. Selley, *Applied Sedimentology* (Academic, London, 1988), pp. 64–65.
[11] D. R. Nelson, M. Rubinstein, and F. Spaepen, Philos. Mag. A **46**, 105 (1982).
[12] M. Ammi, D. Bideau, J. P. Troadec, F. Ropital, and G.

Thomas, Solid State Commun. **55**, 1 (1985).
[13] G. Barker and M. Grimsom, New Sci. **126** (5), 37 (1990).
[14] A. Rosato, K. J. Strandburg, F. Prinz, and R. H. Swendsen, Phys. Rev. Lett. **58**, 1038 (1987).
[15] A. Rosato, K. J. Strandburg, F. Prinz, and R. H. Swendsen, Powder Technol. **49**, 59 (1986).
[16] G. W. Baxter and R. P. Behringer, Physica D **51**, 465 (1991).
[17] R. R. Berg, *Reservoir Sandstones* (Prentice-Hall, Englewood Cliffs, NJ, 1986).
[18] D. P. Haughey and G. S. G. Beveridge, Can. J. Chem. Eng. **47**, 130 (1969).
[19] G. C. Kuczynski, D. P. Uskovic, H. Palmour III, and M. M. Ristic, *Sintering '85* (Plenum, New York, 1987).
[20] R. B. Bjorklund and B. Liedberg, J. Chem. Soc. Chem. Commun. 1293 (1986).
[21] S. P. Armes and B. Vincent, J. Chem. Soc. Chem. Commun. 288 (1987).
[22] S. P. Armes, J. F. Miller, and B. Vincent, J. Colloid Interface Sci. **118**, 410 (1987).
[23] S. P. Armes and M. Aldissi, Polymer **31**, 569 (1990).
[24] S. P. Armes, M. Aldissi, S. Agnew, and S. Gottesfeld, Mol. Cryst. Liq. Cryst. **190**, 63 (1990).
[25] M. J. Vold, Phys. Chem. **63**, 1608 (1959).
[26] The flow of a collection of aspherical particles has been modeled using a cellular automaton in Ref. [16].
[27] K. Binder, *Monte Carlo Methods in Statistical Mechanics*, 2nd ed. (Springer, Berlin, 1986).
[28] Actually, there are a countably infinite number of angular velocities that will place the particle into the correct final orientation. The choices for the angular velocity are reduced to the set for which the particle will not spin in place. The angular velocity used to propagate the particle is then chosen randomly and with uniform probability from this set.
[29] J. Vieillard-Baron, J. Chem. Phys. **56**, 4729 (1972).
[30] The initial density was not exactly 0.25 in each case because we discretized space.
[31] In Ref. [16] it was observed that, when ellipses are poured out of a container, the particles in the flowing region tend to align parallel to **g**.
[32] P. G. de Gennes, *The Physics of Liquid Crystals* (Clarendon, Oxford, 1974).
[33] D. C. Beard and P. K. Weyl, Bull. Am. Assoc. Petrol. Geol. **57**, 349 (1973).
[34] H. J. Fraser, J. Geol. **43**, 910 (1935).

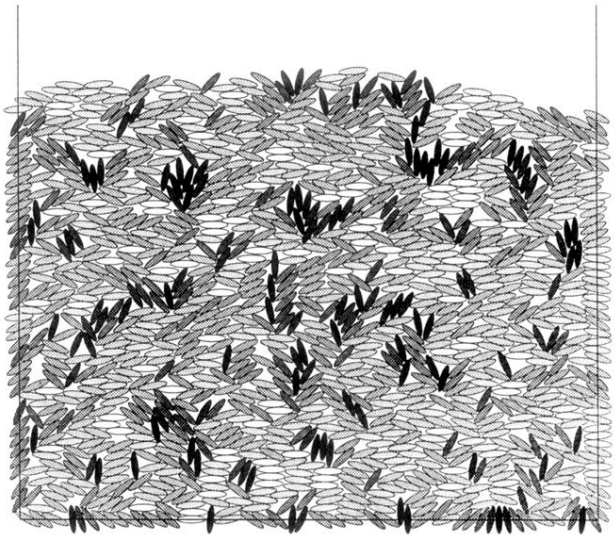

FIG. 1. A packing of 1200 ellipses with $\alpha=4$. The shading of each particle is proportional to $|\theta-\pi/2|$, where $\theta=\pi/2$ is represented by black and $\theta=0$ is represented by white. This shading makes it easier to see oriented domains. The initial density in this simulation was $\gamma=0.25$.

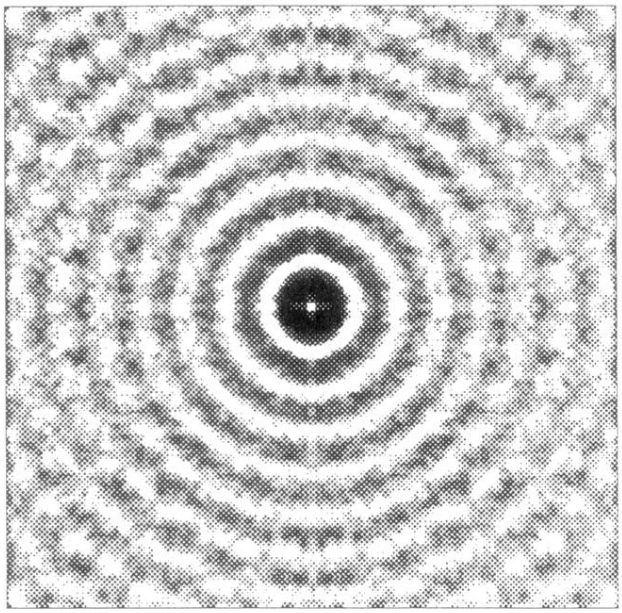

FIG. 3. The scattering pattern for a typical packing of 600 disks. The rings indicate that the packing is polycrystalline. The initial density in this simulation was $\gamma = 0.25$.

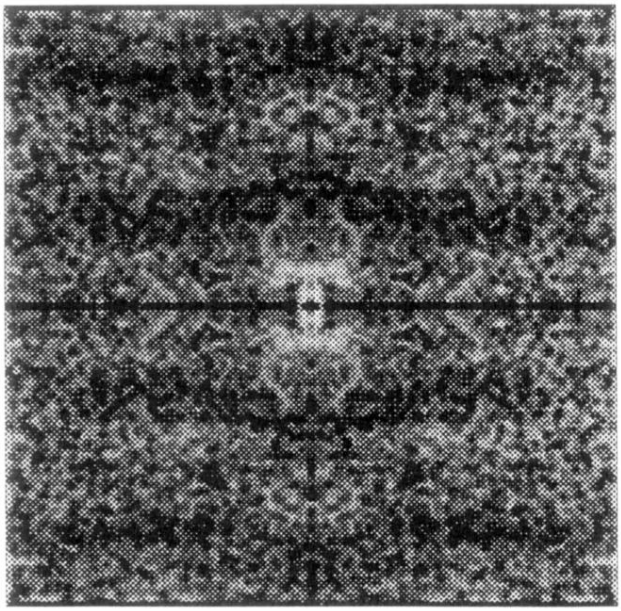

FIG. 4. The scattering pattern for a typical packing of 600 ellipses with aspect ratio $\alpha=8$. This scattering pattern has no structure, indicating that the packing is amorphous. The initial density in this simulation was $\gamma=0.25$.

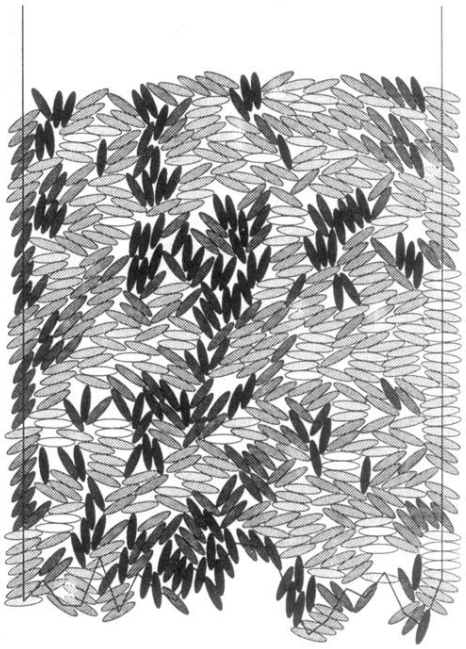

FIG. 9. A packing of 600 particles with $\alpha=4$ in a box with a piecewise linear random bottom. $\mathcal{Q}$ in 0.254 for this packing. The initial density in this simulation was $\gamma=0.1726$.